

Instituto Tecnológico y de Estudios Superiores de Monterrey

Campus Monterrey

School of Engineering and Sciences



Drug delivery dynamics of biopolymer-protein based
nanostructures cues via experimental approach and mathematical
modeling

A thesis presented by:

Luis Ángel Ibarra Sánchez

Submitted to the:

School of Engineering and Sciences

In partial fulfillment of the requirements for the degree of

Master of Science

In

Nanotechnology

Monterrey, Nuevo León. June 7th, 2022

Dedication

To my family, Leobardo Altamira, Socorro Sánchez, Daniela Ibarra, and Leobardo Ibarra, for your endless support on every step that took me to this moment.

To my roomies, Eduardo Ochoa, Erik Najera, Fernanda Díaz, and Brando Morales, for being my foreign family for more than a year and being my company during the last stressful moments in developing this work.

To my best friend, Fernanda Burgos, for all the emotional support despite the distance and the short time available, always present in every good and challenging moment of this master's program.

To Ilse Gaytan, for your long-distance company at Monterrey. Also, for constantly reminding me to trust in my capacities, enjoy the ride, and stay well-hydrated during the hottest days at Monterrey.

To the SAB group, for all the academic and personal support, during the development of this thesis project. Finally, giving a special mention to Rocio, Berenice, Ana Laura, Diana, Edgar, Miguel, Lynette, and Adrian.

Acknowledgments

This project acknowledges at CONACyT, for providing to the student Luis Ángel Ibarra Sánchez with CVU No. 1078456, with maintenance scholarship.

To the Tecnológico de Monterrey, Campus Monterrey, for the provision of scholarship. Additionally, for being the physical space for the development of this project.

To the Centro de Biotecnología FEMSA, for providing the budget to purchase reagents and materials for the development of this project.

To the laboratories from the Centro del Agua para América Latina y el Caribe, for the kind support with materials, equipment, and technical support for the work in this project.

Drug delivery dynamics of biopolymer-protein based nanostructures cues via experimental approach and mathematical modeling

By

Luis Ángel Ibarra Sánchez

Abstract

Respiratory diseases are leading the burden in public health, usually found in the top chart of leading causes of death for many countries. Moreover, COVID-19 has aggravated this situation, having numerous patients with mild to severe symptoms. Besides, lung tissue inflammation and mucus overproduction are critical factors in patients' comorbidity, not only for COVID-19 but also in other pulmonary diseases. In this project, the aim was to integrate the natural therapeutics curcumin (with a studied anti-inflammatory effect) and papain (a proteolytic enzyme used for mucus degradation) into a drug delivery nanostructure to administer intranasally. To reach this goal, curcumin was encapsulated in alginate particles with the emulsion-gelation method, obtaining an encapsulation efficiency of 81.23%. Also, curcumin particles showed a mean size of 500.8 nm, and a surface charge of -23.5 mV. Nonetheless, more studies are required to fully understand the emulsion system to obtain smaller and less disperse particles. Also, bioavailability and efficacy test are required to confirm feasibility of the project. In summary, nanoencapsulation in alginate via emulsion-gelation method has shown promising results for enhancing the curcumin solubility, bioavailability, and stability, to develop more efficient pulmonary treatments against inflammation.

List of figures

Figure 1. Schematic of different drug delivery nanostructures used for the treatment of respiratory diseases.	11
Figure 2. Principal synthesis methods, targeted diseases, and administration routes of polymeric nanoparticles for respiratory diseases treatment.	11
Figure 3. Nano-in-microstructure of curcumin-loaded alginate nanoparticles and co-loaded with papain in pectin microcapsules for lung inflammation and mucus overproduction treatment.	14
Figure 4. Curcumin release kinetics in PBS at 37 °C and pH of 7.4. Different mathematical models were tested to describe the release behavior of curcumin-loaded alginate particles.	22
Figure 5. FT-IR analysis of particles. Alg Gel (green) = alginate gel prepared by ionotropic gelation, Empty-Alg (red) = alginate particles synthesized by emulsion-gelation method without the addition of curcumin, Cur-Alg = curcumin-loaded alginate particles. Transmittance spectrums were displaced in 50% to have a better visualization of the curves.	23
 Figure A1. Curcumin standard curve at 427 nm. The range of concentrations used was 10 µg/mL to 1 µg/mL, the measurements were made in triplicated.	33
Figure A2. Curcumin standard curve at 427 nm. The range of concentrations used was 1 µg/mL to 0.1 µg/mL, the measurements were made in triplicated.	34

List of tables

Table 1. Experimental design for the development of curcumin-loaded alginate particles synthesis via emulsion-gelation method.	16
Table 2. Synthesized curcumin-alginate particles characterization by DLS.	19
Table 3. Curcumin encapsulation efficiencies in particles as a function of alginate and surfactant concentration in emulsion-gelation method	20
Table 4. Drug release mathematical model constants fitted for curcumin loaded-alginate particles	21

Contents

Abstract	5
List of figures	6
List of tables	7
Chapter 1. Introduction	9
Chapter 2. Methodology	15
2.1 Materials	15
2.2 Curcumin-loaded alginate nanoparticle synthesis by emulsion gelation method	15
2.3 Nanoparticle characterization.....	16
2.3.1 Mean nanoparticle hydrodynamic size and Z potential determination using DLS	16
2.3.2 Encapsulation efficiency of curcumin-loaded alginate particles via emulsion-gelation.....	16
2.3.3 Release profile of curcumin from loaded alginate particles	17
2.3.4 FT-IR spectrum of curcumin-loaded alginate particles	18
Chapter 3. Results & Discussion.....	18
3.1 Effects of alginate and surfactant concentration in curcumin loaded particles synthesis.....	18
3.2 Curcumin encapsulation efficiency in alginate by the emulsion-gelation method	20
3.3 Release profile of curcumin-loaded alginate particles.....	20
3.4 FT-IR analysis of curcumin-loaded alginate particles.....	22
Chapter 4. Conclusions & Future Perspectives	24
4.1 Conclusions	24
4.2 Future perspectives.....	24
References.....	26
Appendix A. Supplementary material.....	32
Methodology supplementary material.....	32
Appendix B. Papers publications & conference slides	35
Curriculum vitae.....	39

Chapter 1. Introduction

Pulmonary diseases represent one of the major burdens in public health. According to the revision made by Ahmad & Anderson pulmonary diseases still appear in the leading causes of death in the United States. By 2020 recent COVID-19, chronic lower respiratory diseases, influenza and pneumonia, and chronic lower respiratory diseases appear to be the 3rd, 9th, and 6th principal causes of death, respectively (Ahmad & Anderson, 2021). In the UK, 24% of the deaths at hospitals corresponds to respiratory diseases, being influenza and pneumonia the principal hospital admission cause, closely followed by chronic lower respiratory diseases (Naser et al., 2021). Also, workplace exposure to different substances and particles can contribute to the development, and therefore, increasing the number of cases of chronic lower respiratory diseases. This situation is significantly worsened in low- and middle-income countries, where respiratory diseases can appear as the leading hospitalization and death cause, motivated by the inadequate research, prevention, and management of these diseases (Viegi et al., 2020; Zeng et al., 2022).

In respiratory diseases, there are present two major symptoms, the inflammation of the pulmonary epithelium tissue, and the overproduction and secretion of mucus. Different studies have focused on understanding the mechanisms behind the pulmonary epithelium inflammation, finding that different exterior hazards can trigger the activation of immune cells, hence, starting a mediators' secretion to prepare the body to fight against those hazards, therefore, resulting in epithelium inflammation (Duvall et al., 2017). This inflammation mediator's expression is composed of different cytokines, being the principal pro-inflammatory cytokines: TNF- α , a group of interleukins (IL-1 β , IL-6, IL-8), and IFN γ (Moldoveanu et al., 2009). Despite inflammation being a natural immune response of the body against different pulmonary hazards (such as pathogens, contaminants, and particles), prolonged inflammation can result in a significant reduction in tissue regeneration and damage, consequently promoting the development of other pathologies (Robb et al., 2016).

Moreover, during the cytokine expression, not only inflammatory response is activated but goblet epithelial cells are stimulated to produce more mucus to trap and avoid the advance of pathogens, toxins, and particles (Loxham et al., 2014). Mucus is mainly composed of water (around 95%), numerous proteins composing the network that confers its gel structure (the principal mucus proteins are MUC2, MUC5AC, and MUC5B), and ions (Demouveau et al., 2018). The mucus accomplishes two major roles, the protection of the epithelium tissue by forming a gel coating, and the cleaning of the epithelial tissue by removing dead cells, microorganisms, and other substances (Hansson, 2019). In healthy patients the number of cells secreting mucins is lower, but as the immune response is activated and cytokines promote the inflammatory response and the increase in production and release of mucins results in a thicker and more viscous gel layer (Williams et al., 2006). When the mucus is hypersecreted other complications may appear due to the restriction in oxygen exchange in the lungs, therefore, decreasing the tissue

regeneration capacity, and the increase in chances of co-infections (Shukla et al., 2020; Tan et al., 2022).

Even though how problematic the prolonged inflammatory and mucus hypersecretion response can result, actual treatment still presents limited effectiveness due to the first pass metabolism, and the increase in mucus production difficulties in local administration (Barnes & Stockley, 2005; Collnot et al., 2012). Therefore, novel treatments are required in the treatment of respiratory diseases.

Nanomedicine, the use of different nanostructures to carry and target release therapeutics, has presented a new panorama in respiratory diseases. Some nanostructures used in pulmonary drug diseases are polymeric nanoparticles, polymeric micelles, liposomes, lipid-based nanoparticles, dendrimers, and exosomes; but those therapeutics have mainly been focused on cancer, antiviral, and antibacterial treatment of pulmonary diseases (Ibarra-Sánchez et al., 2022; Melchor-Martínez et al., 2021). In **Figure 1**. Schematic of different drug delivery nanostructures used for the treatment of respiratory diseases., are presented a schematic for different nanostructures focused on the treatment of pulmonary diseases, and some of the targeted diseases. Among the different types of nanostructures for drug delivery, polymeric nanoparticles are distinguished by their high stability, tunable structure and properties, and variety of synthesis methods (Abasian et al., 2020). In **Figure 2**. Principal synthesis methods, targeted diseases, and administration routes of polymeric nanoparticles for respiratory diseases treatment., are presented different diseases in which polymeric nanoparticles were tested for therapy, also the most relevant synthesis methods are presented in a small scheme and remarking the administration routes used in different studies. Still, biocompatibility, biodegradability, and cytotoxicity still representing a challenge for those types of particles (Spireescu et al., 2021).

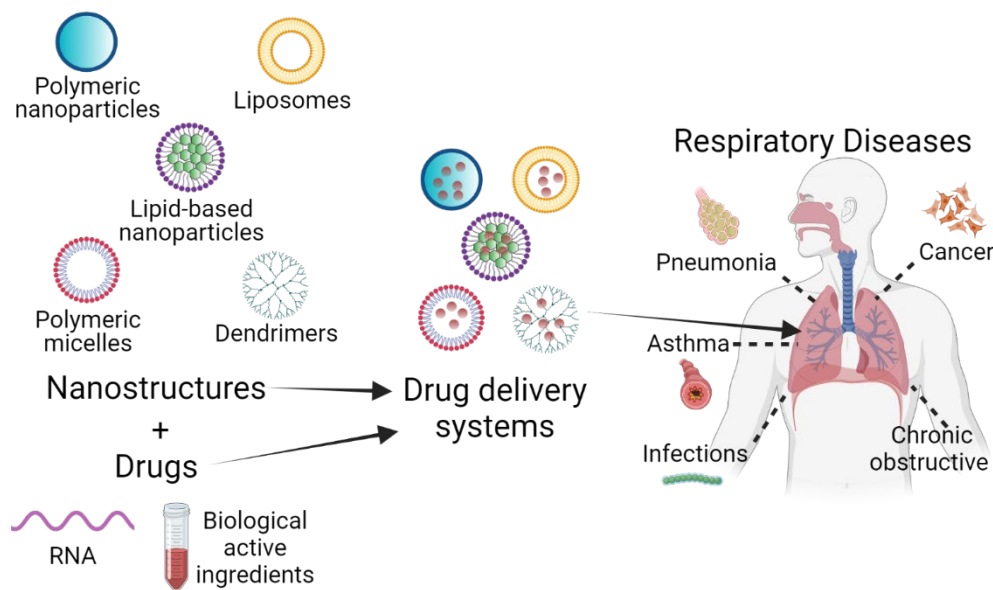
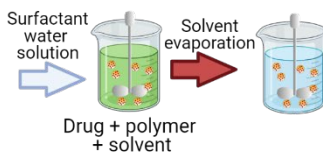


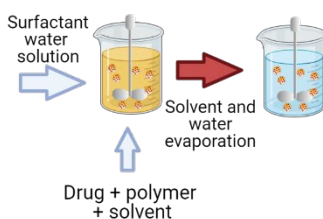
Figure 1. Schematic of different drug delivery nanostructures used for the treatment of respiratory diseases.

Fabrication methods:

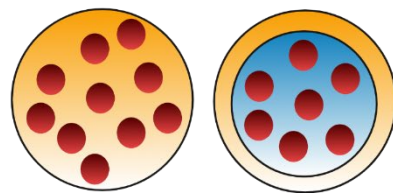
Emulsification/solvent evaporation



Nanoprecipitation



Polymeric nanoparticles



Nanosphere Nanocapsule

Targeted respiratory diseases:

- + Lung cancer
- + Pulmonary hypertension
- + Lung inflammation
- + MERS-CoV and SARS-CoV-2

Administration routes:

- + Intravenous
- + Inhalation
- + Oral

Figure 2. Principal synthesis methods, targeted diseases, and administration routes of polymeric nanoparticles for respiratory diseases treatment.

To overcome the polymeric nanoparticles' limitations mentioned before, many studies have focused on the use of biopolymers, these polymers are based on biological molecules found in different organisms, those molecules are naturally produced by plants, animals, and microorganisms (Song et al., 2020). Due to their origin, biopolymers are conferred with natural biocompatibility, biodegradability, and reduced cytotoxicity especially compared to synthetic polymers (Simionescu &

Ivanov, 2016). Among the variety of biopolymers found in the literature for drug delivery systems, two polysaccharides are distinguished by their wide number of studies used as polymeric nanoparticles matrix or to coat other particles: alginate and pectin (Luo & Wang, 2014).

Alginate is a polysaccharide present in marine algae and brown seaweeds, comprising around 15-20% of its composition (Saravana et al., 2018). Its chemical structure is based on two types of blocks, a 1-4 linked α -L-guluronic (G-block), and β -D-mannuronic acid (M-block), presenting an aleatory linear arrangement of G-G, M-M, and G-M blocks (Pragya et al., 2021). Alginate can easily form gels in presence of divalent ions such as Ca^{2+} , Sr^{2+} , Zn^{2+} , and Ba^{2+} ; this process occurs due to a dimeric association of G-G alginate blocks around the divalent ions, forming a structure usually known as “egg-box junctions” (Tahtat et al., 2017). Due to its origin, it has proven to have good biological properties, water solubility, and is a low-cost material (Taemeh et al., 2020). Therefore, alginate has been widely studied for drug delivery systems, especially loaded with water-soluble drugs, and gene delivery (Huh et al., 2017; Patra et al., 2018). But also, alginate electronegativity allows its electrostatic interaction with positively charged particles, therefore, has been used as a stabilizer coating for a variety of nanostructures (Barclay et al., 2019).

On the other side, pectin is a polysaccharide present in the cellular wall, this confers pectin to a wide range of sources and makes it a cheap resource. Its chemical structure presents a great number of 1-4 linked α -D-galactosyluronic acid residues, some of them are esterified with methyl conferring different properties depending on the grade of esterified acid residues in its chain (Freitas et al., 2021). Those acid residues confer pectin with the capacity with a gelling property. Therefore, historically speaking, pectin has been used in the food industry as an additive gelling agent, and food stabilizer (Adetunji et al., 2017). In recent years, research studies have focused on the development of pectin-based drug delivery systems, gene delivery, for wound healing purposes, and delivering in mucosal regions, especially for the drug delivery in the gastrointestinal tract (Carrion et al., 2021; Rascón-Chu et al., 2019). The combination of biopolymers with nanotechnology can open the chance of using different biologically active agents that previously were limited due to their physicochemical properties. That is the case for curcumin, a polyphenol presents in *Curcuma longa* roots, those roots have been used as a spice called turmeric with a characteristic yellow-orange and crystalline powder used as a food coloring (Caillaud et al., 2020). Curcumin has shown promising therapeutic properties as an anticancer, antimicrobial, antioxidant, neuroprotective, and anti-inflammatory activity (Amalraj et al., 2017). Curcumin can present anti-inflammatory effect by interfering in the expression of the $\text{Nf-}\kappa\text{B}$ gene, this gene is one of the principal activators of $\text{TNF-}\alpha$ cytokine. Since $\text{TNF-}\alpha$ is one of the principal cytokines during inflammatory response, the interference of curcumin with $\text{Nf-}\kappa\text{B}$ results in a downregulation of inflammatory response (Hewlings & Kalman, 2017). Nonetheless, its poor water solubility, and therefore poor bioavailability, has limited its application for therapy in its free form (Stohs et al., 2020). In order to enhance its solubility and stability under physiological conditions, curcumin has been integrated into a variety

of nanostructures, such as gold nanoparticles (Muniyappan et al., 2021), liposomes for cancer therapy (Feng et al., 2017), polymeric nanoparticles (Trigo Gutierrez et al., 2017), and nanoemulsions for pulmonary delivery of curcumin (al ayoub et al., 2019).

Successful deliver treatment to the lung tissue can be accomplished by direct administration to the lungs via inhalation. Yet, in lung diseases, when mucus over secretion is present, administration can be challenging. Therefore, different drug delivery systems have been studied to avoid the mucus barrier and deliver the therapeutic (Khutoryanskiy, 2018). As an example, papain, a protease enzyme extracted from *Carica papaya* has been used for this purpose. It can be considered safe for oral intake considering its presence in fruits as papaya (Leichner et al., 2017). Is a simple enzyme, containing 212 amino acid residue chains, with and hydrophobic core, with a optimal performance at neutral pH. Nonetheless, it can show activity in a wide range of pH (Hitesh et al., 2012). Papain has found a wide range of applications; as a meat tenderizing, in dairy industry, used in the drug production processes, and even being used as a therapeutic (Tacias-Pascacio et al., 2021). Therefore, papain has the potential to affect the mucus protein structure, helping in its removal and facilitating the diffusion of nanoparticles in is way to epithelial tissue.

This work aims to develop and characterize a biopolymeric nanostructure for the treatment of airway inflammation and mucus overproduction, by the nanoencapsulation of curcumin (as an anti-inflammatory agent) in alginate nanoparticles using the emulsion-gelation agent, and the microencapsulation of nanoparticles and papain (as a mucus degradation agent) in ionic gelated pectin microcapsules to enhance particle deposition in lungs. In Figure 4, is presented a schematic representation of the proposed nano-in-microstructure for the treatment of lung inflammation and mucus overproduction.

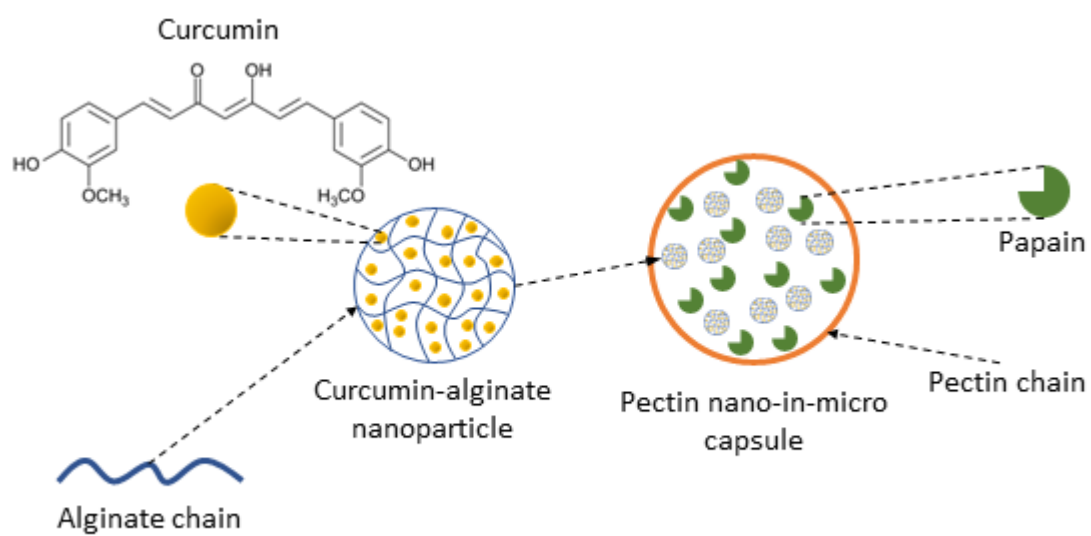


Figure 3. Nano-in-microstructure of curcumin-loaded alginate nanoparticles and co-loaded with papain in pectin microcapsules for lung inflammation and mucus overproduction treatment.

Chapter 2. Methodology

2.1 Materials

Sodium alginate, Tween® 80 suitable for cell culture, Curcumin from *Curcuma longa* (Turmeric), were purchased from Sigma-Aldrich México. Calcium chloride anhydrous analytical grade was purchased from CTR Scientific México. High purity dichloromethane HPLC/Spectro grade was purchased from M TEDIA United States. The rest of the reagents used were analytical grade.

2.2 Curcumin-loaded alginate nanoparticle synthesis by emulsion gelation method

Curcumin-loaded alginate particles were synthesized by the emulsion-gelation method, following the procedure proposed by Kiarnesi et al. with some modifications (Kiarnesi et al., 2021). In brief, the aqueous phase consisted of an aqueous solution of sodium alginate, a weighted amount of alginate was mixed with enough miliQ water to reach the desired concentration, and magnetically stirred (1500 rpm) at room temperature (27 °C) for 3 h prior use. The oily phase consisted of 1 mg/mL of curcumin solution in dichloromethane with the required volume of Tween 80 as a surfactant to reach the desired concentration. And a solution of 3% (w/v) of CaCl₂ in miliQ water was used as the gelation agent for the alginate (magnetically stirred at 1500 rpm for 3 h at 27 °C).

The emulsion was conducted in glass vials of 40 mL, first 5 mL of the oily phase was placed in a clean glass vial, then it was mechanically mixed at 3000 rpm using a vortex mixer. Next, 4 mL of the alginate solution was added drop wisely with the aid of a Kd Scientific syringe pump 100 (using 5 mL BD Plastipak syringe) at a rate of 80 mL/h. Once the total volume of alginate was added and emulsified, the gelation started with the dropwise addition of 1 mL of the CaCl₂ solution at a rate of 20 mL/h.

After emulsion-gelation, the glass vials were kept under magnetically stirring at 1500 rpm at room temperature for 12 h to evaporate the solvent. Following, the resultant aqueous suspension was transferred to Falcon tubes to start 4 washing cycles to remove free curcumin, and the excess of Tween 80, alginate, and CaCl₂. The washing cycles consisted of centrifugation at 4000 rpm at 4 °C for 10 minutes to precipitate the particles, and then, carefully removing and collect the supernatant. Between cycles, particles were resuspended in 5 mL of miliQ water with the aid of a vortex mixer at 3000 rpm. To further characterize, after nanoparticle washing cycles, 1 mL of sample was stored at 4 °C for DLS measurement, and the rest was frozen at -70 °C for 12 h prior lyophilization.

To test the effect of the alginate concentration and the surfactant concentration on the particle synthesis, various experiments were conducted according to **Table 1**. Each experiment was conducted in triplicate.

Table 1. Experimental design for the development of curcumin-loaded alginate particles synthesis via emulsion-gelation method.

		Tween 80 concentration (% v/v)		
		1% (-1)	2% (0)	3% (+1)
Alginate concentration (% w/v)	0.1% (-1)	-1/-1	-1/0	-1/+1
	0.5% (0)	0/-1	0/0	0/+1
	1.0% (+1)	+1/-1	+1/0	+1/+1

2.3 Nanoparticle characterization

To determine the effectiveness of the emulsion-gelation method for the synthesis of the curcumin-loaded alginate particles, different techniques were used to evaluate the physical properties of the particles, as well as their release profile. In the next sections the methodologies followed to characterize the samples are described.

2.3.1 Mean nanoparticle hydrodynamic size and Z potential determination using DLS

The particles hydrodynamic size distribution was measured using the Dynamic Light Scattering (DLS) technique, using a Z-Sizer Nano (Malvern) with a laser of 423 nm at a fixed backscattered angle of 173°, using a stabilizing temperature of 25 °C. After washing cycles, and prior the lyophilization, 1 mL of sample was taken, sonicated for 1 min, and then diluted in miliQ water using a factor of 1:8. Next, 800 µL of the sample was placed into disposable cuvettes. Each sample has a single measurement with an automatic number of runs. To determine the Z potential of the particles it was used the deep immersion adaptor of the equipment, temperature, number of measurements, and number of runs conserved the configuration used for particle distribution.

2.3.2 Encapsulation efficiency of curcumin-loaded alginate particles via emulsion-gelation

The efficiency of curcumin encapsulation was determined by an indirect method. In brief, during the washing cycles the supernatants were collected, and then the supernatants were gauged to a known volume of 50 mL using miliQ water. Then, a standard curve was prepared for the curcumin (refer to **Figure A1**) using a DR 5000 Hach spectrophotometer at a maximum absorbance λ of 427 nm. Following, 100 µL of the gauged supernatant sample was taken and diluted using a factor of 10:1 (dilution: supernatant), to finally place 1 mL of diluted sample into a disposable acrylic cuvette. Each measurement was done in triplicate. Finally, the Encapsulation Efficiency (EE) was computed using **Eq. 1**.

$$EE = \left(\frac{I - C \times V \times DF}{I} \right) \times 100 \quad \text{Eq. 1}$$

Where EE is the encapsulation efficiency of the emulsion-gelation method expressed as a percentage of the initial mass of curcumin added; I is the initial amount of curcumin in the oily phase expressed in μg ; C is the concentration ($\mu g/mL$) of curcumin measured the diluted sample of gauged supernatant; V the final volume of supernatant after gauging (mL), and DF is the dilution factor used prior measurements in the spectrophotometer.

2.3.3 Release profile of curcumin from loaded alginate particles

The release profile of curcumin-loaded alginate particles was performed in the standard medium, PBS at pH 7.4, the experimental conditions were 37 °C, and magnetic stirring of 20 rpm to simulate the number of breaths per minute of a human in resting condition (Russo et al., 2017). In detail, a weighted amount of lyophilized curcumin-loaded particles was suspended in 3 mL of PBS solution, then the suspension was placed into a cellulose tubing dialysis membrane with a molecular weight cut-off of 14-12 kDa. Then, the charged cellulose membrane was placed into 27 mL of PBS (to get a final volume of 30 mL) at the mentioned conditions. Then, 3 aliquots of 1 mL were taken for their further measurement using UV-vis spectrophotometer and replaced with a fresh medium to maintain the sink conditions. The aliquots were taken at intervals of 0, 1, 2, 4, 8, 12, 24, 48, and 72 h. The experiment was conducted in triplicate.

In addition, the data obtained was adjusted using the most common release kinetics models: zero order, first order, Higuchi's, and Korsmeyer-Peppas models were tested (**Eq. 5**, **Eq. 3**, **Eq. 4**, **Eq. 5**, respectively). The best-fitted constants and R^2 values for each model were reported.

$$Q_t = Q_0 + K_0 t \quad \text{Eq. 2}$$

Where Q_t is the mass of drug released at time t , Q_0 corresponds to the initial amount of drug, which is 0 in most cases, and K_0 is the release constant with units of concentration/time.

$$C = C_{eq} \cdot (1 - e^{-K \cdot t}) \quad \text{Eq. 3}$$

For the first order kinetics, C represents the amount of drug released at time t , C_{eq} is the amount of drug when the system is at equilibrium, and K is the first order kinetic constant in units of time to the minus one.

$$Q_t = K_H \cdot t^{1/2} \quad \text{Eq. 4}$$

In the case of Higuchi's model, Q_t is the amount of drug released at time t , and K_H is the Higuchi's release rate constant.

$$\frac{M_t}{M_\infty} = K \cdot t^n \quad \text{Eq. 5}$$

And finally, in the Korsmeyer-Peppas model, M_t/M_∞ is the fraction of drug released at time t , K is the Korsmeyer-Peppas release rate constant, and n is the release exponent, which is usually related to the release mechanism for controlled release of polymeric systems (Sreedharan & Singh, 2019).

2.3.4 FT-IR spectrum of curcumin-loaded alginate particles

The aim was to evaluate the interaction between the nanoparticle components; therefore, FT-IR analysis was done in a Perkin-Elmer Frontier FT-IR Spectrometer equipped with the universal ATR sampling accessory. In brief, the sample preparation consisted of after synthesis of curcumin-loaded alginate particles, the sample was lyophilized to obtain a powder of the nanostructure for FT-IR analysis. Also, empty emulsion-gelated alginate particles, and simple gelled alginate particles were prepared and analyzed to obtain their spectrum using a step size of 1 cm^{-1} from 4000 to 400 cm^{-1} and 64 scans.

Chapter 3. Results & Discussion

To develop an effective delivery method of curcumin to the lung epithelium tissue, there were prepared alginate particles loaded with curcumin via the emulsion-gelation method. Two main variables were investigated, the concentration of alginate solution (the amount of alginate available), and the surfactant concentration of the oily phase (forming a micelle around the disperse phase and stabilizing the emulsion). Whereas curcumin amount, emulsion speed, addition rate, and ionic crosslinker concentration kept constant. The results from particle characterization for the different treatments are presented in the next sections.

3.1 Effects of alginate and surfactant concentration in curcumin loaded particles synthesis

The results according to the experimental design (refer to **Table 1**) are presented in **Table 2**. The mean hydrodynamic size and z potential were determined by dynamic light scattering (DLS). According to the measurements, the mean hydrodynamic diameter varied from 500.8 nm up to 2851.0 nm. The combination of parameters 1% v/v of Tween 80 and 0.1% w/v of sodium alginate resulted in the smallest hydrodynamic diameter of 500.8 nm, these particles still presented a greater hydrodynamic diameter than those obtained by Kiarnesi et al. using its water in oil emulsion, being oil-to-water phase ratio, agitation speed, and oil phase component (olive oil for the mentioned work) the main differences from the ones synthesized in this project (Kiarnesi et al., 2021). It can be observed that the concentration of alginate in the aqueous phase leads to higher particle size, this can be attributed to changes in the viscosity of the aqueous phase, modifying the rheological behavior of the emulsion, and reducing the capacity of disperse phase to divide into smaller

aqueous droplets. Also, the increase of alginate available for CaCl_2 gelation bonds can lead to a significant aggregation of droplets during the gelation process. Similar behavior has been observed in works such as Mokhtari et al. synthesizing alginate particles by emulsion/internal gelation method for peppermint phenolic extract encapsulation (Mokhtari et al., 2017). Additionally, it can be observed that the increase of surfactant v/v% in the oil phase suggests an increase in the size of the particle. This occur when the excess surfactant goes into the formation of aggregation of surfactant particles, and finally increases the size of the disperse phase droplets (Sarheed et al., 2021). Moreover, the agitation energy administered to the systems during synthesis can be a relevant factor influencing the particle size, for example, Sheir et al. obtained alginate-chitosan particles below 300 nm by the sonication of the precursors during the gelation (Sheir et al., 2021).

In this study, the concentration of the gelation agent was fixed at 3% w/v to provide excess Ca^{2+} , to ensure the full gelation of the alginate available in the aqueous phase. Notably, other studies where ionic gelated alginate particles were synthesized, suggested that the concentration of Ca^{2+} ions can also affect the particle size (Thomas et al., 2020), representing an important factor to review in future research to obtain smaller particles than the ones obtained in this work.

The surface charge of particles round from -13.9 mV to -27.4 mV, this was expected due to the electronegativity of alginate hydrogels. Other works of alginate particles have presented similar Z potentials, such as the ones used by Bakhshi et al. to encapsulate immunoglobulin in alginate by ionic gelation with Z potentials from -26 to -36 mV (Bakhshi et al., 2017). The strong electronegativity of synthesized particles can have a positive effect on nanoparticle stability, due to the repulsive electrostatic forces.

Table 2. Synthesized curcumin-alginate particles characterization by DLS.

Alginate (w/v%)	Tween 80 (v/v%)	Particle mean size (nm)	Pdl	Z potential (mV)
0.1	1	500.8 ± 127	0.603	-23.5 ± 2.3
0.5	1	894.3 ± 289	0.926	-21.0 ± 1.7
1.0	1	911.9 ± 69	0.704	-22.7 ± 1.3
0.1	2	992.0 ± 284	0.790	-16.5 ± 1.1
0.5	2	1623.3 ± 144	0.671	-13.9 ± 1.0
1.0	2	1543.0 ± 128	0.551	-18.8 ± 0.6
0.1	3	1716.0 ± 198	1.000	-23.1 ± 0.3
0.5	3	2277.0 ± 690	0.861	-24.1 ± 3.7
1.0	3	2851.0 ± 172	0.997	-27.4 ± 5.1

DLS: dynamic light scattering

3.2 Curcumin encapsulation efficiency in alginate by the emulsion-gelation method

The encapsulation efficiency was found to vary from 20.39% to 81.23%. The maximum encapsulation efficiency corresponds to the combination of 1.0% of alginate (w/v) and 1% of surfactant (v/v). The results suggest that the amount of alginate does not have a direct effect on the encapsulation efficiency. Otherwise, the amount of curcumin entrapped can be related to the amount of surfactant used, showing that more surfactant results in less curcumin being entrapped. This can be due to the saturation of disperse phase surface with the surfactant, blocking the path of curcumin to the gelled alginate particles. Other studies using alginate in nanoparticle composition have obtained similar curcumin encapsulation efficiencies; for example, encapsulation efficiency of 76.06% was obtained using zein particles double-coated with sodium caseinate/sodium alginate (Liu et al., 2019); Sorasitthiyanukarn et al. reached an encapsulation efficiency of 85% for curcumin diethyl diglutarate using alginate/chitosan particles synthesized by a similar O/W emulsion and ionotropic gelation (Sorasitthiyanukarn et al. 2019); and an encapsulation efficiency of 95% was obtained with bovine serum albumin/alginate-modified Fe₃O₄ particles (Amani et al., 2019) while using different matrixes have obtained encapsulation efficiencies from 50% to 100% for systems like liposomes and cubosomes synthesized by reverse phase evaporation (Chang et al., 2021), and encapsulation efficiency of 67% for microfluidic PLGA nanoencapsulation of curcumin (Lababidi et al., 2019).

Table 3. Curcumin encapsulation efficiencies in particles as a function of alginate and surfactant concentration in emulsion-gelation method

Alginate (w/v%)	Tween 80 (v/v%)	Encapsulation efficiency (%)
0.1	1	80.10 ± 0.95
0.5	1	78.64 ± 0.35
1.0	1	81.23 ± 1.63
0.1	2	60.33 ± 2.02
0.5	2	66.05 ± 2.66
1.0	2	63.86 ± 2.03
0.1	3	22.10 ± 2.10
0.5	3	20.39 ± 0.14
1.0	3	25.35 ± 2.10

UV-vis: UV-visible spectrophotometry.

3.3 Release profile of curcumin-loaded alginate particles

Understanding the drug release kinetics is an important factor in the development of drug delivery systems. To evaluate our particles kinetics a standard drug release assay was performed under the typical conditions, using PBS at pH 7.4 at a

temperature of 37 °C. Low agitation was used to model the mechanical conditions in the lungs for patients in rest conditions. In **Figure 4** the experimental release profile is presented, it can be observed an initial burst of curcumin release at the first 2 hours, followed by a sustained release for the following hours up to 72 h. This type of release is usually present in drug release mainly conducted by diffusion. To confirm that, and for a better understanding of kinetics, different mathematical models were tested to describe the experimental behavior obtained. Four mathematical models were tested, zero order, first order, Higuchi's model, and Korsmeyer-Peppas model; the constant values and R^2 values obtained after curve fitting are presented in **Table 4**. The model that better describes the system was Korsmeyer-Peppas, presenting an R^2 value of 0.9294, this can be confirmed in the model graphic presented in **Figure 4**. The Q_0 coefficient value (7.440674) can be related to the curcumin equilibrium concentration for the system, while the n exponent value (0.093324) can be correlated to the dominant release mechanism, that according to the literature, an $n < 0.43$ is related to a Fickian-diffusive driven process (Siepmann & Peppas, 2012). This type of release can be suitable for prolonged administration of curcumin to the tissue.

Table 4. Drug release mathematical model constants fitted for curcumin loaded-alginate particles

Model	Constant values		R ²
Zero order	Q_0	K_0	
	6.621735	0.084599	0.5953
First order	C_{eq}	K	
	9.681764	1.295099	0.8519
Higuchi	K_H		
	1.827163		0.3818
Korsmeyer-Peppas	Q_0	n	
	7.440674	0.093324	0.9294

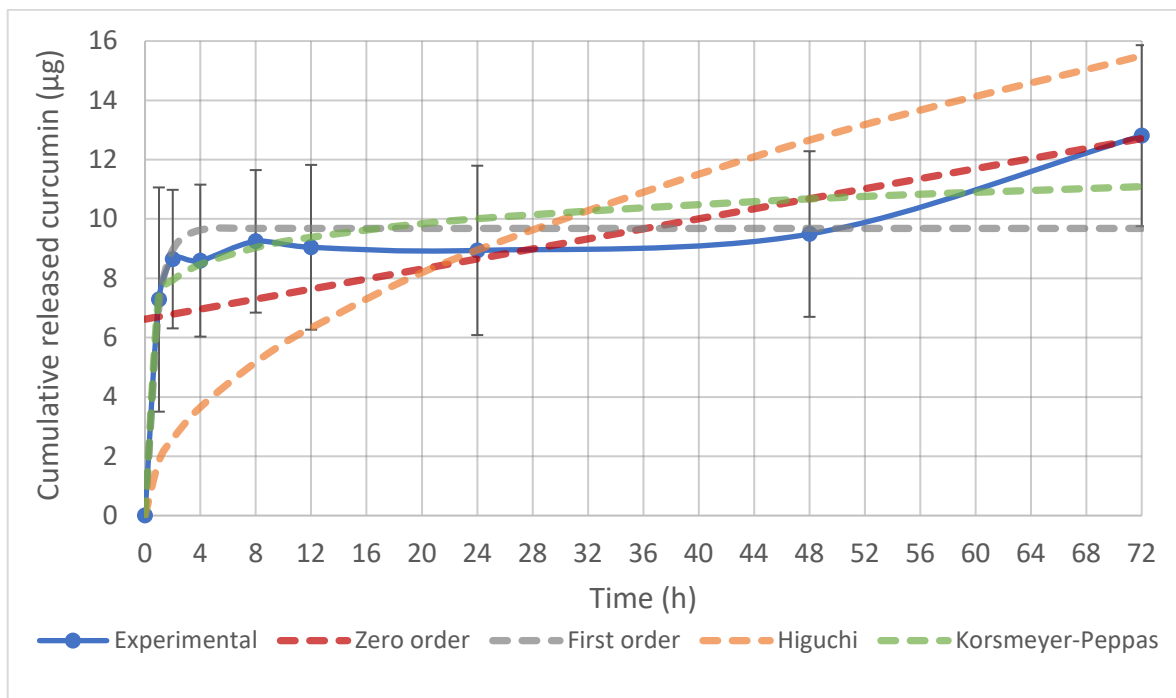


Figure 4. Curcumin release kinetics in PBS at 37 °C and pH of 7.4. Different mathematical models were tested to describe the release behavior of curcumin-loaded alginate particles.

3.4 FT-IR analysis of curcumin-loaded alginate particles

To investigate the possibility of an interaction between alginate and curcumin for the encapsulation mechanism a FT-IR was conducted. In **Figure 5** the spectrums for different samples are presented. In green is shown the spectrum for alginate gel particles synthesized by the dropwise addition of CaCl_2 solution to a 0.1% solution of sodium alginate. The spectrum shows an O–H stretching vibration band at the range from 3600 up to 3200 cm^{-1} which can be attributed to the remaining water in the sample. The absorption peaks at 1595 cm^{-1} and 1416 cm^{-1} correspond to asymmetric and symmetrical elongations of carboxylate groups of the alginate polymer, respectively; and the symmetrical deformation band of the COO^- group appears around 1027 cm^{-1} . Results are comparable to the alginate gel spectrum obtained by Siqueira et al., where characteristic peaks were reported at 1594 cm^{-1} , 1410 cm^{-1} , and 1424 cm^{-1} (Siqueira et al., 2019), small differences in peaks can be attributed to the difference in equipment, and precursor reagents.

Red spectra correspond to alginate particles synthesized by the full emulsion-gelation method used in this study by omitting the addition of curcumin in the dichloromethane. Spectra remains like the alginate gel spectrum, but an absorption band appears around 1676 cm^{-1} to 1779 cm^{-1} , with its peak at 1738 cm^{-1} . Also, one of the characteristic peaks of alginate suffered a small displacement to 1591 cm^{-1} , this small differences in spectra can be attributed to the presence of surfactant in the surface of the alginate particles. Accordingly, to the Tween 80 FT-IR spectra showed

by Choudhury et al., where a Tween 80-Span 80 complex spectrum showed a maximum absorption peak at 1742 cm^{-1} , corresponding to C=O bonds stretch (Choudhury et al., 2013). However, the small ratio of surfactant to alginate, resulted in the apparition of a small peak at 1738 cm^{-1} for our sample.

The blue spectra correspond to the curcumin-loaded alginate particles synthesized with the same alginate concentration (0.1% w/v) and surfactant concentration (1% v/v). Here curcumin's characteristic peaks were found at 3394 cm^{-1} ; 1624 cm^{-1} , 1585 cm^{-1} , and 1513 cm^{-1} ; 1425 cm^{-1} , and 1276 cm^{-1} ; and 961 cm^{-1} . Therefore, the curcumin spectra are comparable to the one obtained by Chen et al. (Chen et al., 2015). Additionally, we can observe that the alginate spectra are covered by curcumin, even though, the small peak attributed to the surfactant still present in the sample, denoting the presence of alginate particles. Results suggest the interaction of curcumin with the nanostructure, nonetheless, more characterization is required to confirm the interaction between nanostructure components and the curcumin.

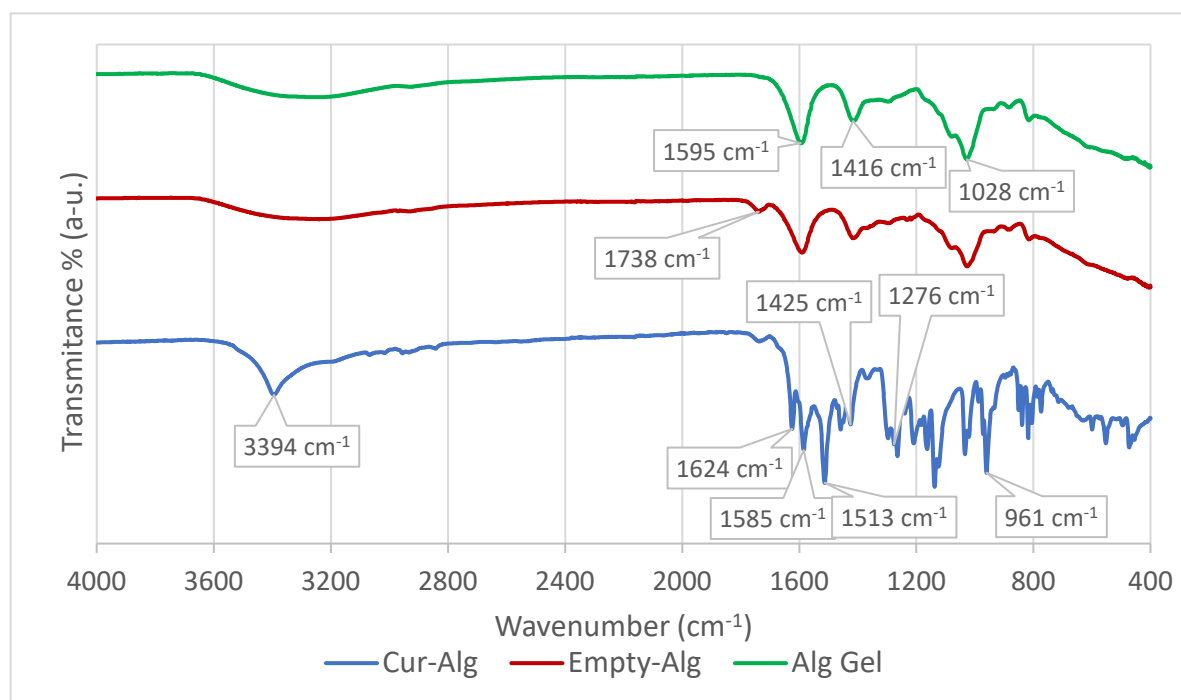


Figure 5. FT-IR analysis of particles. Alg Gel (green) = alginate gel prepared by ionotropic gelation, Empty-Alg (red) = alginate particles synthesized by emulsion-gelation method without the addition of curcumin, Cur-Alg = curcumin-loaded alginate particles. Transmittance spectrums were displaced in 50% to have a better visualization of the curves.

Chapter 4. Conclusions & Future Perspectives

4.1 Conclusions

Pulmonary diseases still represent a major burden on public health. Lung tissue inflammation and mucus overproduction are common symptoms of a variety of pulmonary diseases such as COVID-19, asthma, chronic obstructive pulmonary diseases, pneumonia, influenza, and many other. However, treatment of those symptoms is not a trivial task, due to the different metabolism mechanisms that inhibit or reduce the therapeutic effect of traditional treatments. This work explored the possibility of using a biopolymeric-based nanostructure to encapsulate curcumin, an anti-inflammatory molecule, and deliver it to the lung epithelium to treat tissue inflammation. Different conditions were tested to obtain the best results in particle size, z potential, and encapsulation efficiency of curcumin when alginate particles are synthesized by emulsion-gelation method. From the different combinations in alginate and surfactant concentration, a high encapsulation efficiency reached up to 81%, being comparable to other nanostructures such as liposomes and micelles. Even though, particle size still represents an improvement area, the best results presented particles with a mean hydrodynamic diameter of around 500 nm, which is still above the ideal particle size range of 100 to 200 nm. Release kinetics described by the mathematical model of Korsmeyer-Peppas showed a Fickian-diffusion drug release process which can ensure a prolonged release of curcumin through time, this is desirable due to the translation to smaller administration dosages and simpler administration schedules. In summary, the encapsulation method presented here remains a promising method to synthesize curcumin-loaded particles in the treatment of pulmonary diseases.

4.2 Future perspectives

The reach of this work allows to understand some of the interactions among the components of this system, specifically, alginate concentration and surfactant concentration. High encapsulation efficiency and the slow and sustained release of curcumin highlights the capacity of the system proposed for enhanced curcumin delivery using biopolymeric matrices.

Even though, other important aspects still required to investigate, such as the efficacy and cytotoxicity tests, those are essential aspects to review in novel therapeutics development. The size of the particles still above the definition of nanoparticles, therefore, it is recommended to run more test by varying other parameters such as the agitation speed, concentration of ionic solution, and the ratio between the disperse and continuous phase. Those parameters can be critical to obtain particles below 200 nm in size. Also, due to the time restrictions, SEM

micrography still pending to characterize the real size and morphology of the synthesized particles.

Additionally, in this work was proposed that the double encapsulation of particles with papain inside of pectin microstructures can be used for the double purpose of enhancing the particle deposition and mucus degradation in lungs. To reach this goal, it was proposed to use a microfluidic droplet generator that allow to microencapsulate curcumin and papain inside of pectin capsules using ethanol and ionic gelation. Therefore, the droplet generator design was prepared using AutoCAD. Then, the devices were constructed using laser cutting and soft lithography techniques. Initial tests on the basic functionality of the device were made to test its quality. However, time was a critical factor that affect the reach of this phase of the project. Future work in this should focus in obtaining a fully functional microfluidic droplet generator. In order that goal, computational modeling can be used to make and initial screening of the proposed designs. What is more, the use of laser cutting can be a limiting factor to resolution in design engraving, therefore, other fabrication methods should be revised.

In summary, this project comprises the first steps to develop a pulmonary drug delivery nanostructure.

References

- Abasian, P., Ghanavati, S., Rahebi, S., Nouri Khorasani, S., & Khalili, S. (2020). Polymeric nanocarriers in targeted drug delivery systems: A review. *Polymers for Advanced Technologies*, 31(12), 2939–2954. <https://doi.org/10.1002/pat.5031>
- Adetunji, L. R., Adekunle, A., Orsat, V., & Raghavan, V. (2017). Advances in the pectin production process using novel extraction techniques: A review. *Food Hydrocolloids*, 62, 239–250. <https://doi.org/10.1016/j.foodhyd.2016.08.015>
- Ahmad, F. B., & Anderson, R. N. (2021). The Leading Causes of Death in the US for 2020. *JAMA*, 325(18), 1829. <https://doi.org/10.1001/jama.2021.5469>
- al ayoub, Yuosef., Gopalan, R. C., Najafzadeh, M., Mohammad, M. A., Anderson, D., Paradkar, A., & Assi, K. H. (2019). Development and evaluation of nanoemulsion and microsuspension formulations of curcuminoids for lung delivery with a novel approach to understanding the aerosol performance of nanoparticles. *International Journal of Pharmaceutics*, 557, 254–263. <https://doi.org/10.1016/j.ijpharm.2018.12.042>
- Amalraj, A., Pius, A., Gopi, S., & Gopi, S. (2017). Biological activities of curcuminoids, other biomolecules from turmeric and their derivatives – A review. *Journal of Traditional and Complementary Medicine*, 7(2), 205–233. <https://doi.org/10.1016/j.jtcme.2016.05.005>
- Amani, S., Mohamadnia, Z., & Mahdavi, A. (2019). pH-responsive hybrid magnetic polyelectrolyte complex based on alginate/BSA as efficient nanocarrier for curcumin encapsulation and delivery. *International Journal of Biological Macromolecules*, 141, 1258–1270. <https://doi.org/10.1016/j.ijbiomac.2019.09.048>
- Bakhshi, M., Ebrahimi, F., Nazarian, S., Zargan, J., Behzadi, F., & Gariz, D. S. (2017). Nano-encapsulation of chicken immunoglobulin (IgY) in sodium alginate nanoparticles: In vitro characterization. *Biologicals*, 49, 69–75. <https://doi.org/10.1016/j.biologicals.2017.06.002>
- Barclay, T. G., Day, C. M., Petrovsky, N., & Garg, S. (2019). Review of polysaccharide particle-based functional drug delivery. *Carbohydrate Polymers*, 221, 94–112. <https://doi.org/10.1016/j.carbpol.2019.05.067>
- Barnes, P. J., & Stockley, R. A. (2005). COPD: current therapeutic interventions and future approaches. *European Respiratory Journal*, 25(6), 1084–1106. <https://doi.org/10.1183/09031936.05.00139104>

- Caillaud, M., Aung Myo, Y. P., McKiver, B. D., Warncke, U. O., Thompson, D., Mann, J., del Fabbro, E., Desmoulière, A., Billet, F., & Damaj, M. I. (2020). Key Developments in the Potential of Curcumin for the Treatment of Peripheral Neuropathies. *Antioxidants*, 9(10), 950. <https://doi.org/10.3390/antiox9100950>
- Chang, C., Meikle, T. G., Drummond, C. J., Yang, Y., & Conn, C. E. (2021). Comparison of cubosomes and liposomes for the encapsulation and delivery of curcumin. *Soft Matter*, 17(12), 3306–3313. <https://doi.org/10.1039/D0SM01655A>
- Chen, X., Zou, L.-Q., Niu, J., Liu, W., Peng, S.-F., & Liu, C.-M. (2015). The Stability, Sustained Release and Cellular Antioxidant Activity of Curcumin Nanoliposomes. *Molecules*, 20(8), 14293–14311. <https://doi.org/10.3390/molecules200814293>
- Choudhury, S. R., Mandal, A., Chakravorty, D., Gopal, M., & Goswami, A. (2013). Evaluation of physicochemical properties, and antimicrobial efficacy of monoclinic sulfur-nanocolloid. *Journal of Nanoparticle Research*, 15(4), 1491. <https://doi.org/10.1007/s11051-013-1491-y>
- Collnot, E.-M., Ali, H., & Lehr, C.-M. (2012). Nano- and microparticulate drug carriers for targeting of the inflamed intestinal mucosa. *Journal of Controlled Release*, 161(2), 235–246. <https://doi.org/10.1016/j.jconrel.2012.01.028>
- Demouveau, B., Gouyer, V., Gottrand, F., Narita, T., & Desseyn, J.-L. (2018). Gel-forming mucin interactome drives mucus viscoelasticity. *Advances in Colloid and Interface Science*, 252, 69–82. <https://doi.org/10.1016/j.cis.2017.12.005>
- Duvall, M. G., Bruggemann, T. R., & Levy, B. D. (2017). Bronchoprotective mechanisms for specialized pro-resolving mediators in the resolution of lung inflammation. *Molecular Aspects of Medicine*, 58, 44–56. <https://doi.org/10.1016/j.mam.2017.04.003>
- Feng, T., Wei, Y., Lee, R. J., & Zhao, L. (2017). Liposomal curcumin and its application in cancer. *International Journal of Nanomedicine*, Volume 12, 6027–6044. <https://doi.org/10.2147/IJN.S132434>
- Freitas, C. M. P., Coimbra, J. S. R., Souza, V. G. L., & Sousa, R. C. S. (2021). Structure and Applications of Pectin in Food, Biomedical, and Pharmaceutical Industry: A Review. *Coatings*, 11(8), 922. <https://doi.org/10.3390/coatings11080922>
- Hansson, G. C. (2019). Mucus and mucins in diseases of the intestinal and respiratory tracts. *Journal of Internal Medicine*, 285(5), 479–490. <https://doi.org/10.1111/joim.12910>

- Hewlings, S., & Kalman, D. (2017). Curcumin: A Review of Its Effects on Human Health. *Foods*, 6(10), 92. <https://doi.org/10.3390/foods6100092>
- Hitesh, P., Manojbhai, B. N., Mayuri, B. A., Ashvinkumar, D. D., & Kiraben, D. v. (2012). Extraction and Application of Papain Enzyme on Degradation of Drug. *International Journal of Pharmacy and Biological Sciences*, 2(3), 113–115.
- Huh, M. S., Lee, E. J., Koo, H., Yhee, J. Y., Oh, K. S., Son, S., Lee, S., Kim, S. H., Kwon, I. C., & Kim, K. (2017). Polysaccharide-based Nanoparticles for Gene Delivery. In *Polymeric Gene Delivery Systems* (pp. 65–83). https://doi.org/10.1007/978-3-319-77866-2_3
- Ibarra-Sánchez, L. Á., Gámez-Méndez, A., Martínez-Ruiz, M., Nájera-Martínez, E. F., Morales-Flores, B. A., Melchor-Martínez, E. M., Sosa-Hernández, J. E., Parra-Saldívar, R., & Iqbal, H. M. N. (2022). Nanostructures for drug delivery in respiratory diseases therapeutics: Revision of current trends and its comparative analysis. *Journal of Drug Delivery Science and Technology*, 70, 103219. <https://doi.org/10.1016/j.jddst.2022.103219>
- Khutoryanskiy, V. v. (2018). Beyond PEGylation: Alternative surface-modification of nanoparticles with mucus-inert biomaterials. *Advanced Drug Delivery Reviews*, 124, 140–149. <https://doi.org/10.1016/j.addr.2017.07.015>
- Kiarnesi, S., Solouk, A., Saber-Samandari, S., Keshel, S. H., & Pasbakhsh, P. (2021). Alginate nanoparticles as ocular drug delivery carriers. *Journal of Drug Delivery Science and Technology*, 66(102889). <https://doi.org/https://doi.org/10.1016/j.jddst.2021.102889>
- Lababidi, N., Sigal, V., Koenneke, A., Schwarzkopf, K., Manz, A., & Schneider, M. (2019). Microfluidics as tool to prepare size-tunable PLGA nanoparticles with high curcumin encapsulation for efficient mucus penetration. *Beilstein Journal of Nanotechnology*, 10, 2280–2293. <https://doi.org/10.3762/bjnano.10.220>
- Leichner, C., Menzel, C., Laffleur, F., & Bernkop-Schnürch, A. (2017). Development and in vitro characterization of a papain loaded mucolytic self-emulsifying drug delivery system (SEDDS). *International Journal of Pharmaceutics*, 530(1–2), 346–353. <https://doi.org/10.1016/j.ijpharm.2017.08.059>
- Liu, Q., Jing, Y., Han, C., Zhang, H., & Tian, Y. (2019). Encapsulation of curcumin in zein/ caseinate/sodium alginate nanoparticles with improved physicochemical and controlled release properties. *Food Hydrocolloids*, 93, 432–442. <https://doi.org/10.1016/j.foodhyd.2019.02.003>

- Loxham, M., Davies, D. E., & Blume, C. (2014). Epithelial function and dysfunction in asthma. *Clinical & Experimental Allergy*, 44(11), 1299–1313. <https://doi.org/10.1111/cea.12309>
- Luo, Y., & Wang, Q. (2014). Recent development of chitosan-based polyelectrolyte complexes with natural polysaccharides for drug delivery. *International Journal of Biological Macromolecules*, 64, 353–367. <https://doi.org/10.1016/j.ijbiomac.2013.12.017>
- Melchor-Martínez, E. M., Torres Castillo, N. E., Macias-Garbett, R., Lucero-Saucedo, S. L., Parra-Saldívar, R., & Sosa-Hernández, J. E. (2021). Modern World Applications for Nano-Bio Materials: Tissue Engineering and COVID-19. *Frontiers in Bioengineering and Biotechnology*, 9. <https://doi.org/10.3389/fbioe.2021.597958>
- Mokhtari, S., Jafari, S. M., & Assadpour, E. (2017). Development of a nutraceutical nano-delivery system through emulsification/internal gelation of alginate. *Food Chemistry*, 229, 286–295. <https://doi.org/10.1016/j.foodchem.2017.02.071>
- Moldoveanu, B., Otmishi, P., Jani, P., Walker, J., Sarmiento, X., Guardiola, J., Saad, M., & Yu, J. (2009). Inflammatory mechanisms in the lung. *Journal of Inflammation Research*, 2, 1–11.
- Muniyappan, N., Pandeewaran, M., & Amalraj, A. (2021). Green synthesis of gold nanoparticles using *Curcuma pseudomontana* isolated curcumin: Its characterization, antimicrobial, antioxidant and anti-inflammatory activities. *Environmental Chemistry and Ecotoxicology*, 3, 117–124. <https://doi.org/10.1016/j.enceco.2021.01.002>
- Naser, A. Y., Mansour, M. M., Alanazi, A. F. R., Sabha, O., Alwafi, H., Jalal, Z., Paudyal, V., Dairi, M. S., Salawati, E. M., Alqahtan, J. S., Alaamri, S., & Mustafa Ali, M. K. (2021). Hospital admission trends due to respiratory diseases in England and Wales between 1999 and 2019: an ecologic study. *BMC Pulmonary Medicine*, 21(1), 356. <https://doi.org/10.1186/s12890-021-01736-8>
- Patra, J. K., Das, G., Fraceto, L. F., Campos, E. V. R., Rodriguez-Torres, M. del P., Acosta-Torres, L. S., Diaz-Torres, L. A., Grillo, R., Swamy, M. K., Sharma, S., Habtemariam, S., & Shin, H.-S. (2018). Nano based drug delivery systems: recent developments and future prospects. *Journal of Nanobiotechnology*, 16(1), 71. <https://doi.org/10.1186/s12951-018-0392-8>
- Pragya, A., Mutalik, S., Younas, M. W., Pang, S.-K., So, P.-K., Wang, F., Zheng, Z., & Noor, N. (2021). Dynamic cross-linking of an alginate–acrylamide tough hydrogel system: time-resolved in situ mapping of gel self-assembly. *RSC Advances*, 11(18), 10710–10726. <https://doi.org/10.1039/D0RA09210J>

- Robb, C. T., Regan, K. H., Dorward, D. A., & Rossi, A. G. (2016). Key mechanisms governing resolution of lung inflammation. *Seminars in Immunopathology*, 38(4), 425–448. <https://doi.org/10.1007/s00281-016-0560-6>
- Russo, M. A., Santarelli, D. M., & O'Rourke, D. (2017). The physiological effects of slow breathing in the healthy human. *Breathe*, 13(4), 298–309. <https://doi.org/10.1183/20734735.009817>
- Saravana, P. S., Cho, Y.-N., Woo, H.-C., & Chun, B.-S. (2018). Green and efficient extraction of polysaccharides from brown seaweed by adding deep eutectic solvent in subcritical water hydrolysis. *Journal of Cleaner Production*, 198, 1474–1484. <https://doi.org/10.1016/j.jclepro.2018.07.151>
- Sarheed, O., Dibi, M., Ramesh, K. V. R. N. S., & Drechsler, M. (2021). Fabrication of Alginate-Based O/W Nanoemulsions for Transdermal Drug Delivery of Lidocaine: Influence of the Oil Phase and Surfactant. *Molecules*, 26(9), 2556. <https://doi.org/10.3390/molecules26092556>
- Sheir, M. M., Nasra, M. M. A., & Abdallah, O. Y. (2021). Chitosan alginate nanoparticles as a platform for the treatment of diabetic and non-diabetic pressure ulcers: Formulation and in vitro/in vivo evaluation. *International Journal of Pharmaceutics*, 607, 120963. <https://doi.org/10.1016/j.ijpharm.2021.120963>
- Shukla, S. D., Walters, E. H., Simpson, J. L., Keely, S., Wark, P. A. B., O'Toole, R. F., & Hansbro, P. M. (2020). Hypoxia-inducible factor and bacterial infections in chronic obstructive pulmonary disease. *Respirology*, 25(1), 53–63. <https://doi.org/10.1111/resp.13722>
- Siepmann, J., & Peppas, N. A. (2012). Modeling of drug release from delivery systems based on hydroxypropyl methylcellulose (HPMC). *Advanced Drug Delivery Reviews*, 64, 163–174. <https://doi.org/10.1016/j.addr.2012.09.028>
- Simionescu, B. C., & Ivanov, D. (2016). Natural and Synthetic Polymers for Designing Composite Materials. In *Handbook of Bioceramics and Biocomposites* (pp. 233–286). Springer International Publishing. https://doi.org/10.1007/978-3-319-12460-5_11
- Siqueira, P., Siqueira, É., de Lima, A. E., Siqueira, G., Pinzón-Garcia, A. D., Lopes, A. P., Segura, M. E. C., Isaac, A., Pereira, F. V., & Botaro, V. R. (2019). Three-Dimensional Stable Alginate-Nanocellulose Gels for Biomedical Applications: Towards Tunable Mechanical Properties and Cell Growing. *Nanomaterials*, 9(1), 78. <https://doi.org/10.3390/nano9010078>
- Song, J., Winkeljann, B., & Lieleg, O. (2020). Biopolymer-Based Coatings: Promising Strategies to Improve the Biocompatibility and Functionality of Materials Used in Biomedical Engineering. *Advanced Materials Interfaces*, 7(17), 2000850. <https://doi.org/10.1002/admi.202000850>

- Sorasitthyanukarn, F. N., Ratnatilaka Na Bhuket, P., Muangnoi, C., Rojsitthisak, P., & Rojsitthisak, P. (2019). Chitosan/alginate nanoparticles as a promising carrier of novel curcumin diethyl diglutarate. *International Journal of Biological Macromolecules*, 131, 1125–1136. <https://doi.org/10.1016/j.ijbiomac.2019.03.120>
- Spirescu, V. A., Chircov, C., Grumezescu, A. M., & Andronesu, E. (2021). Polymeric Nanoparticles for Antimicrobial Therapies: An up-to-date Overview. *Polymers*, 13(5), 724. <https://doi.org/10.3390/polym13050724>
- Sreedharan, S. M., & Singh, R. (2019). Ciprofloxacin Functionalized Biogenic Gold Nanoflowers as Nanoantibiotics Against Pathogenic Bacterial Strains. *International Journal of Nanomedicine*, Volume 14, 9905–9916. <https://doi.org/10.2147/IJN.S224488>
- Stohs, S. J., Chen, O., Ray, S. D., Ji, J., Bucci, L. R., & Preuss, H. G. (2020). Highly Bioavailable Forms of Curcumin and Promising Avenues for Curcumin-Based Research and Application: A Review. *Molecules*, 25(6), 1397. <https://doi.org/10.3390/molecules25061397>
- Tacias-Pascacio, V. G., Morellon-Sterling, R., Castañeda-Valbuena, D., Berenguer-Murcia, Á., Kamli, M. R., Tavano, O., & Fernandez-Lafuente, R. (2021). Immobilization of papain: A review. *International Journal of Biological Macromolecules*, 188, 94–113. <https://doi.org/10.1016/j.ijbiomac.2021.08.016>
- Taemeh, M. A., Shiravandi, A., Korayem, M. A., & Daemi, H. (2020). Fabrication challenges and trends in biomedical applications of alginate electrospun nanofibers. *Carbohydrate Polymers*, 228, 115419. <https://doi.org/10.1016/j.carbpol.2019.115419>
- Tahtat, D., Bouaicha, M. N., Benamer, S., Nacer-Khodja, A., & Mahlous, M. (2017). Development of alginate gel beads with a potential use in the treatment against acute lead poisoning. *International Journal of Biological Macromolecules*, 105, 1010–1016. <https://doi.org/10.1016/j.ijbiomac.2017.07.137>
- Tan, C. L., Chan, Y., Candasamy, M., Chellian, J., Madheswaran, T., Sakthivel, L. P., Patel, V. K., Chakraborty, A., MacLoughlin, R., Kumar, D., Verma, N., Malya, V., Gupta, P. K., Jha, N. K., Thangavelu, L., Devkota, H. P., Bhatt, S., Prasher, P., Gupta, G., ... Chellappan, D. K. (2022). Unravelling the molecular mechanisms underlying chronic respiratory diseases for the development of novel therapeutics via in vitro experimental models. *European Journal of Pharmacology*, 919, 174821. <https://doi.org/10.1016/j.ejphar.2022.174821>
- Thomas, D., KurienThomas, K., & Latha, M. S. (2020). Preparation and evaluation of alginate nanoparticles prepared by green method for drug

delivery applications. *International Journal of Biological Macromolecules*, 154, 888–895. <https://doi.org/10.1016/j.ijbiomac.2020.03.167>

Trigo Gutierrez, J. K., Zanatta, G. C., Ortega, A. L. M., Balastegui, M. I. C., Sanitá, P. V., Pavarina, A. C., Barbugli, P. A., & de Oliveira Mima, E. G. (2017). Encapsulation of curcumin in polymeric nanoparticles for antimicrobial Photodynamic Therapy. *PLOS ONE*, 12(11), e0187418. <https://doi.org/10.1371/journal.pone.0187418>

Viegi, G., Maio, S., Fasola, S., & Baldacci, S. (2020). Global Burden of Chronic Respiratory Diseases. *Journal of Aerosol Medicine and Pulmonary Drug Delivery*, 33(4), 171–177. <https://doi.org/10.1089/jamp.2019.1576>

Williams, O. W., Sharafkhaneh, A., Kim, V., Dickey, B. F., & Evans, C. M. (2006). Airway Mucus From Production to Secretion. *American Journal of Respiratory Cell and Molecular Biology*, 34(5), 527–536. <https://doi.org/10.1165/rcmb.2005-0436SF>

Zeng, L.-H., Hussain, M., Syed, S. K., Saadullah, M., Jamil, Q., Alqahtani, A. M., Alqahtani, T., Akram, N., Khan, I. A., Parveen, S., Fayyaz, T., Fatima, M., Shaukat, S., Shabbir, N., Fatima, M., Kanwal, A., Barkat, M. Q., & Wu, X. (2022). Revamping of Chronic Respiratory Diseases in Low- and Middle-Income Countries. *Frontiers in Public Health*, 9, 757089. <https://doi.org/10.3389/fpubh.2021.757089>

Appendix A. Supplementary material

Methodology supplementary material

To determine the effective amount of curcumin in the supernatant collected and the released curcumin, a standard curve was prepared at a range of concentrations between 10 µg/mL and 1 µg/mL of curcumin. The resulting standard curve at a maxima wavelength of 427 nm is presented in **Figure A1**.

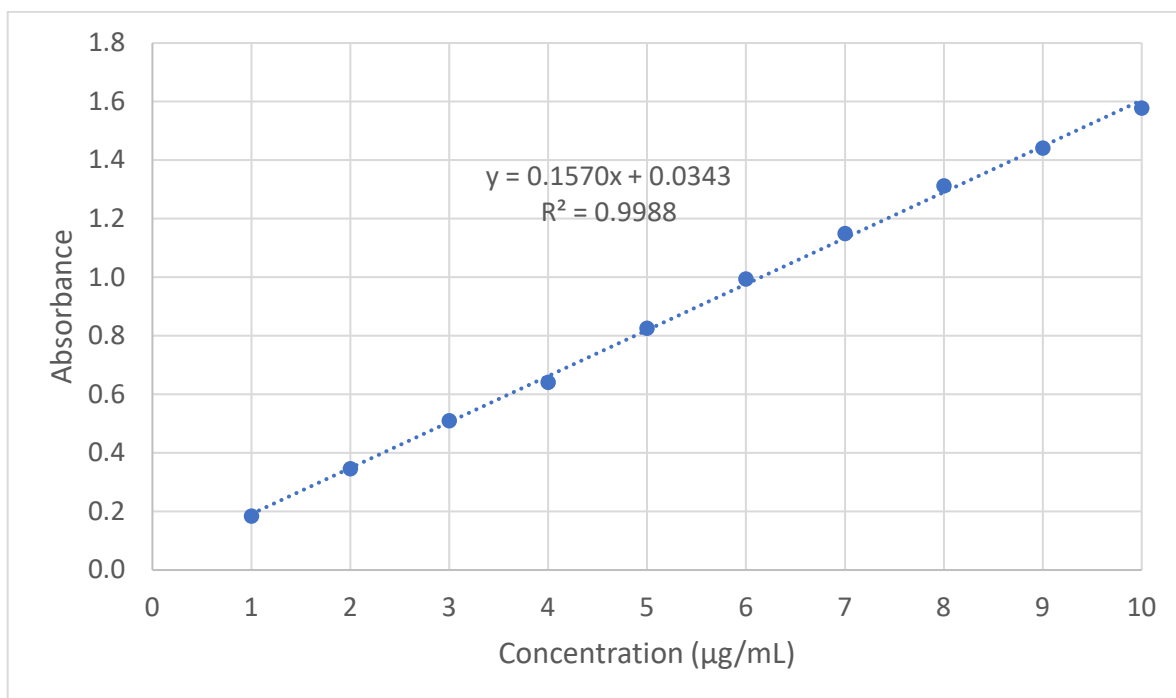


Figure A1. Curcumin standard curve at 427 nm. The range of concentrations used was 10 µg/mL to 1 µg/mL, the measurements were made in triplicated.

During the release profile studies due to the low solubility of curcumin in the media, it was required to prepare a standard curve for lower concentrations. Therefore, it can be observed in Figure A2 the prepared standard curve between 1 µg/mL to 0.1 µg/mL of curcumin. Standard curve was prepared at the standard curve at a maxima wavelength of 427 nm.

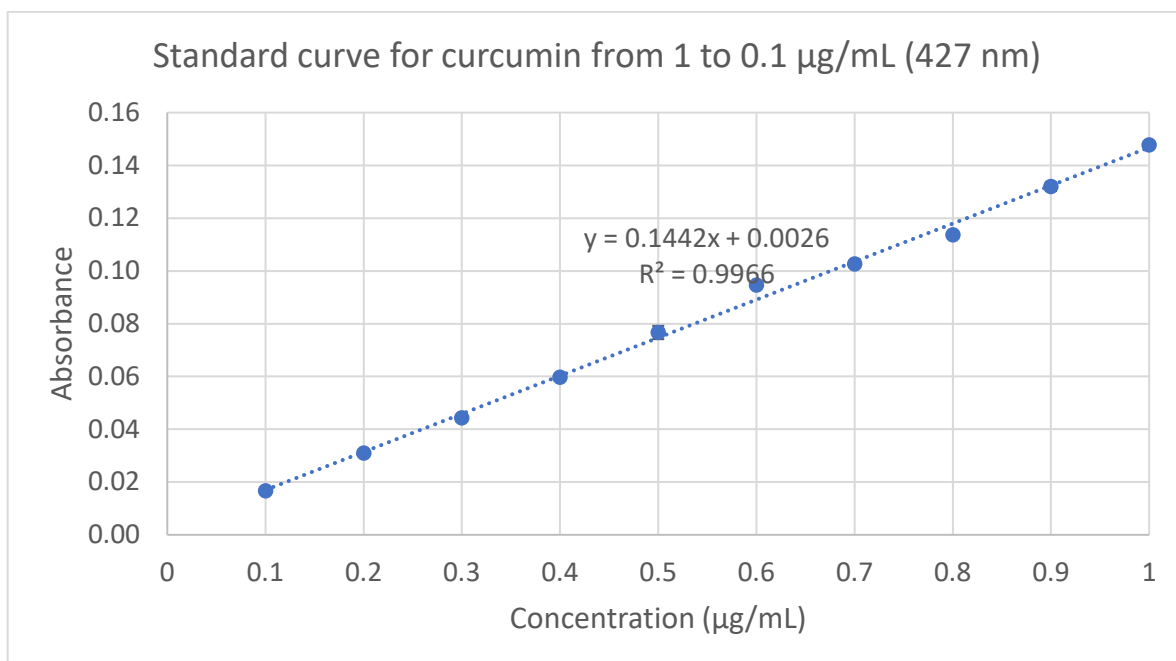
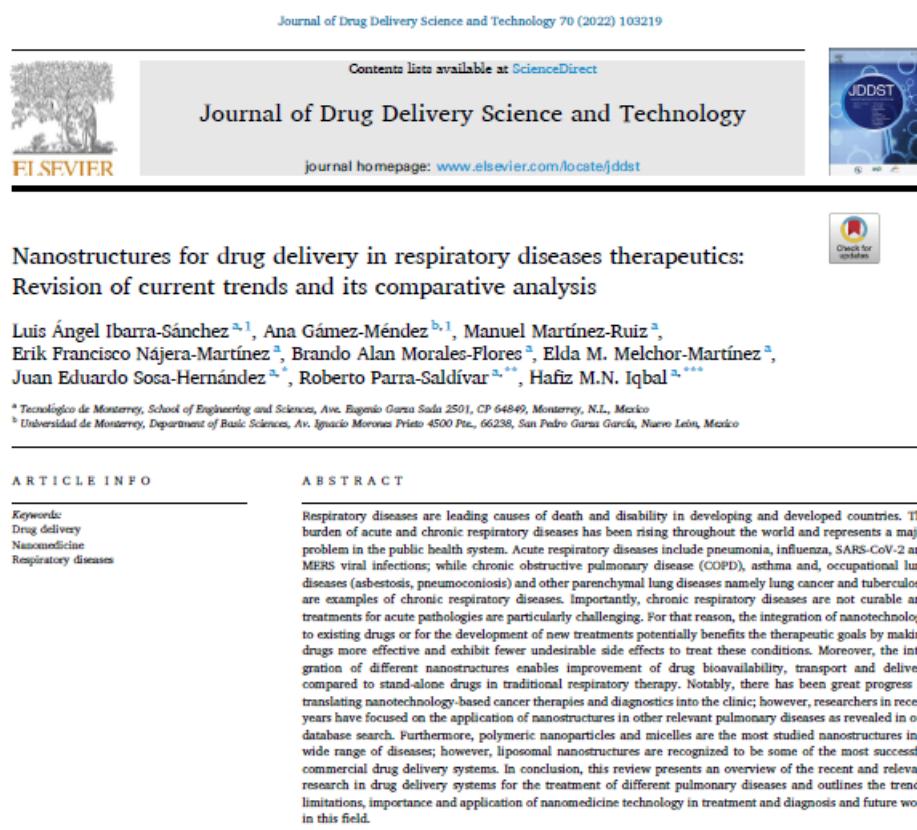


Figure A2. Curcumin standard curve at 427 nm. The range of concentrations used was 1 $\mu\text{g/mL}$ to 0.1 $\mu\text{g/mL}$, the measurements were made in triplicated.

Appendix B. Papers publications & conference slides

Ibarra-Sánchez, L. Á., Gámez-Méndez, A., Martínez-Ruiz, M., Nájera-Martínez, E. F., Morales-Flores, B. A., Melchor-Martínez, E. M., ... & Iqbal, H. M. (2022). Nanostructures for drug delivery in respiratory diseases therapeutics: Revision of current trends and its comparative analysis. *Journal of Drug Delivery Science and Technology*, 103219.



1. Introduction

Pulmonary diseases still remain a critical challenge for actual therapy, according to the report of Heron [1] by the end of 2017 in the United States, chronic lower respiratory diseases and influenza-pneumonia keep a place between the 10 leading causes of death, with a 5.7% and 2.0% of the total deaths per year, respectively. And this situation can get worse in the case of developing countries, where respiratory infections can be found leading the list of the principal

causes of death [2]. Regardless of the number of advances in medicine and development of new treatments, their efficacy in different numbers of pulmonary diseases is still limited [3].

There are a wide range of respiratory diseases and disorders that can vary between chronic, viral infections, fungal and bacterial infection and cancer. Between the historically relevant pulmonary diseases can be found tuberculosis (TB) still having approximately 10 million cases reported by the year of 2017 with a rate of reduction in new cases of 1.5% per year [4], in spite of this reduction in annual cases the actual treatment for latent TB remains a challenge for medicine [5]. It is well known

* Corresponding author.

** Corresponding author.

*** Corresponding author.

E-mail addresses: eduardo.sosa@tec.mx (J.E. Sosa-Hernández), r.parra@tec.mx (R. Parra-Saldivar), hafiz.iqbal@tec.mx (H.M.N. Iqbal).

¹ Authors contributed equally.

<https://doi.org/10.1016/j.jddst.2022.103219>

Received 2 July 2021; Received in revised form 2 February 2022; Accepted 26 February 2022

Available online 5 March 2022

1773-2247/© 2022 Elsevier B.V. All rights reserved.

Advances in a original paper publication: Design of a nano-in-microstructure of alginate-in-pectin particles for curcumin and papain delivery in respiratory diseases (Journal of Drug Delivery Sciences and Technology).

Design of a nano-in-microstructure of alginate-in-pectin particles for curcumin and papain delivery in respiratory diseases

(Journal of Drug Delivery Science and Technology)

Luis Ángel Ibarra-Sánchez ^a, Elda M. Melchor-Martínez¹, Manuel Martínez-Ruiz¹, Juan Eduardo Sosa-Hernández ^{a,b}, Roberto Parra-Saldívar ^a, Hafiz M. N. Iqbal ^a

^a Tecnológico de Monterrey, School of Engineering and Sciences, Ave. Eugenio Garza Sada 2501, CP 64849, Monterrey, N. L., México

^b Corresponding author:

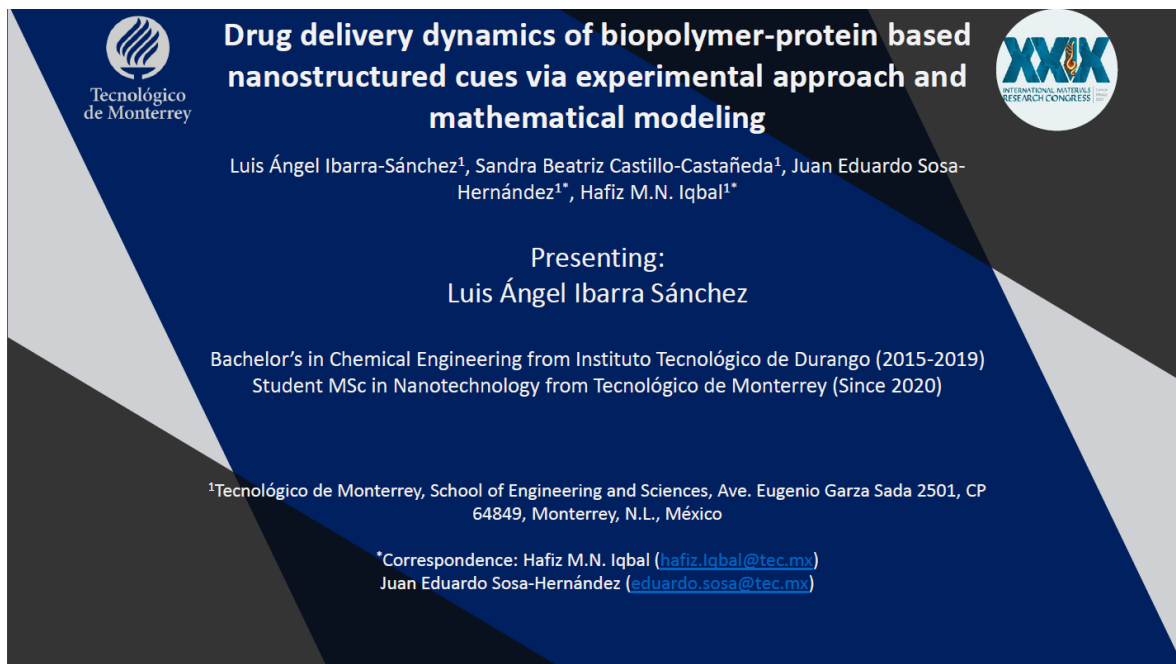
Abstract:


Treatment of pulmonary diseases still represents a challenge for the public health sector, and this has been aggravated by the current COVID-19 pandemic. In this sense, nanotherapeutics have the chance to create new treatment platforms with enhanced bioavailability and compatibility. Herein, in this project curcumin (used as anti-inflammatory agent) was nanoencapsulated with alginate via emulsion-gelation method, and then co-encapsulated with papain using pectin via microfluidic droplet technology. Characterization of curcumin nanoparticles showed a mean particle size of -- nm and a surface charge of --, also obtaining an encapsulation efficiency of -- %, while pectin microparticles showed a mean particle size of -- nm. In conclusion, the developed nano-in-microstructure has the potential to be used in the treatment of pulmonary diseases presenting inflammation and mucus overproduction, even though, in vitro, and in vivo test still required to evaluate biocompatibility and efficacy of the proposed platform.

Keywords:

- Alginate
- Curcumin

Project presentation in the XIX International Materials Research Congress: Drug delivery dynamics of biopolymer-protein based nanostructured cues via experimental approach and mathematical modeling (2021).




Tecnológico
de Monterrey

**Drug delivery dynamics of biopolymer-protein based
nanostructured cues via experimental approach and
mathematical modeling**


Luis Ángel Ibarra-Sánchez¹, Sandra Beatriz Castillo-Castañeda¹, Juan Eduardo Sosa-
Hernández^{1*}, Hafiz M.N. Iqbal^{1*}

Presenting:
Luis Ángel Ibarra Sánchez

Bachelor's in Chemical Engineering from Instituto Tecnológico de Durango (2015-2019)
Student MSc in Nanotechnology from Tecnológico de Monterrey (Since 2020)

¹Tecnológico de Monterrey, School of Engineering and Sciences, Ave. Eugenio Garza Sada 2501, CP
64849, Monterrey, N.L., México

*Correspondence: Hafiz M.N. Iqbal (hafiz.iqbal@tec.mx)
Juan Eduardo Sosa-Hernández (eduardo.sosa@tec.mx)



Coordination and support in UDEM student's residence:

Universidad de Monterrey

Vicerrectoría de Ciencias de la Salud



Programa de Evaluación Final del Programa Académico
IBI

***PROYECTO: IMPLEMENTACIÓN DE DISPOSITIVO
MICROFLUÍDICO PARA APLICACIONES DE
SKIN-ON-A-CHIP***

Asesor:

Ph.D. Ing. Osvaldo Aquines Gutierrez.

Integrantes del Equipo:

Estefany de los Angeles Santini Canul 575155

Marieli Mendez Lugo 575153